ChemComm

COMMUNICATION

View Article Online
View Journal | View Issue

Cite this: *Chem. Commun.*, 2015, **51**, 16964

Received 9th August 2015,
Accepted 29th September 2015

DOI: 10.1039/c5cc06676j

www.rsc.org/chemcomm

Intracellular Zn^{2+} detection with quantum dot-based FLIM nanosensors†

Consuelo Ripoll,[a] Miguel Martin,[b] Mar Roldan,[b] Eva M. Talavera,[a] Angel Orte*[a] and Maria J. Ruedas-Rama*[a]

Fluorescence Lifetime Imaging Microscopy (FLIM) has been employed for the detection of intracellular Zn^{2+} levels, implicated in various signalling pathways, using a family of quantum dot (QD) nanosensors. The sensing mechanism was based on photoinduced electron transfer (PET) between an azacycle receptor group and the QD nanoparticles.

The search for new nanosensors for specific species with minimal local perturbation is of special interest in fields such as chemistry, biology or biomedicine. In particular, the development of appropriate intracellular ion sensors is singularly important because some ions play significant roles in cellular biology.[1] Multimodal fluorescence imaging, based on intensity, lifetime and polarization detection, combined with high spatial resolution enables quantitative readouts that allow for real time monitoring of biological processes through biosensing and bioimaging. One of the most interesting materials for these sensing applications are semiconductor nanocrystals or quantum dots (QDs).[2] QDs have been proposed as an alternative to conventional molecular probes because of their unique optical properties, which are ideally suited for the long-term monitoring of intracellular processes.[3] Among these features, QDs show long photoluminescence (PL) decay times, typically from five to hundreds of nanoseconds, which make them especially interesting for fluorescence lifetime imaging microscopy (FLIM).[4] Most of the published intracellular QD nanosensors are based on changes in the fluorescence intensity when a target ion or molecule interacts with a nanoparticle.[5–7] However, fluorescence intensity-based measurements suffer from uncertainties because they can be altered by fluctuations in the excitation light, the probe concentration and heterogeneities in the optical properties of the medium. As an alternative, the use of time-resolved fluorescence spectroscopy and FLIM imaging can overcome many of these limitations.[8,9] The average PL lifetime of QDs is significantly longer than the lifetime of the cell autofluorescence, which makes QDs easily discernible from the background signal. Although some QD-based luminescence lifetime sensors have been reported for the determination of pH[10] and detection of ions, such as Cl^- or Cu^{2+},[11,12] the advantages of the FLIM technique and its use with QDs as intracellular probes have not yet been extensively exploited.[8] A few examples where QD nanoparticles were employed with FLIM have been described but only for intracellular detection and not for the quantification of the target molecules.[13,14] To date, FLIM has been used as an effective technique only for the quantitative real-time sensing of intracellular pH.[4] Long-decay, near-infrared, emitting QDs have also been applied for *in vivo* pH sensing through FLIM imaging into a nude mouse.[15] These works demonstrated the high sensitivity of these QD-based nanosensors and the great potential of FLIM for intracellular applications.

In this communication, we have shown that this methodology can be extended to the sensing of other ions inside cells. We have focused our attention on Zn^{2+} homeostasis as a crucial intracellular catalytic and signalling mechanism that controls many important cellular events.[16] Deregulation of Zn^{2+} levels can cause several health problems, such as neuronal dysfunction and immunodeficiency. Relevant concentrations of Zn^{2+} range from fM to almost 0.5 mM in some mammalian brain cells. Hence, many efforts are currently in place to develop Zn^{2+} sensors with a wide quantitation range.[17] In this communication, the surface of CdSe/ZnS QDs was properly modified to create a family of intracellular-sensitive Zn^{2+} probes. Two azamacrocycles molecules, cyclen (1,4,7,10-tetraazacyclododecane, **1**) and cyclam (1,4,8,11-tetraazacyclotetradecane, **2**), have been attached by EDC/NHS covalent coupling to the surface of mercaptopropionic acid (MPA) capped-QDs (Fig. 1a, and ESI† for more details), for the preparation of **QD–1** and **QD–2** conjugates. We have employed QDs of two different sizes that emit at 520 ($\mathbf{QD_{520}}$) and 600 nm ($\mathbf{QD_{600}}$). Upon attachment, a proximal nitrogen lone pair acts as

[a] *Department of Physical Chemistry, Faculty of Pharmacy, University of Granada, Campus Cartuja, 18071 Granada, Spain. E-mail: angelort@ugr.es, mjruedas@ugr.es; Tel: +34-958243825, +34-958247887*

[b] *GENYO, Pfizer-University of Granada-Junta de Andalucia Centre for Genomics and Oncological Research, Avda Ilustracion 114, PTS, 18016 Granada, Spain*

† Electronic supplementary information (ESI) available: Experimental details, methods of analysis, Tables S1 and S2, and Fig. S1–S5. See DOI: 10.1039/c5cc06676j

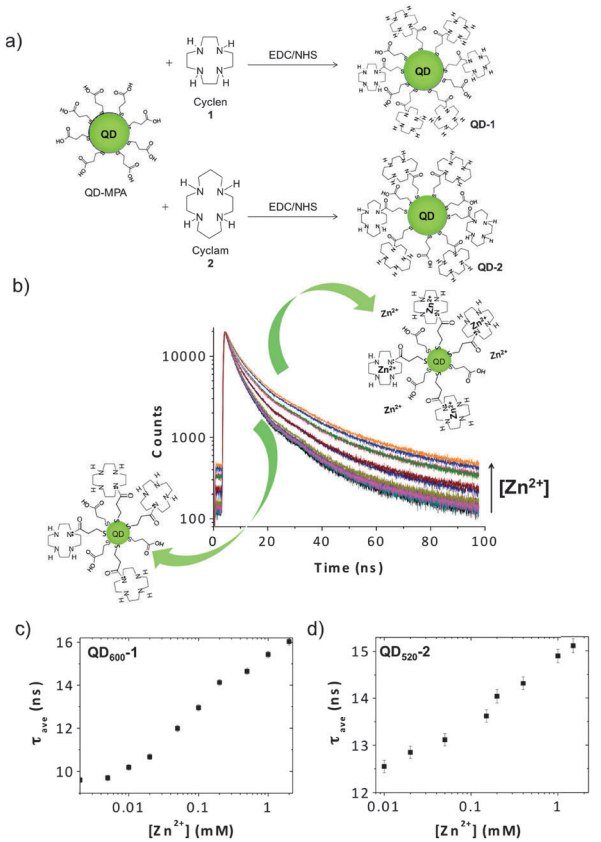

Fig. 1 (a) Scheme of covalent coupling reaction for the formation of the QD–azacycle conjugates. (b) PL decay traces of **QD_{600}–1** conjugates in the presence of 0, 0.001, 0.005, 0.01, 0.05, 0.1, 0.5, and 2 mM of Zn^{2+} (λ_{ex} = 440 nm and λ_{em} = 598 nm, Tris buffer pH 7.2). Average lifetime calculated from the decays for (c) **QD_{600}–1** and (d) **QD_{520}–2** conjugates.

an electron donor to the excited QD, producing a quenching of the PL emission *via* photoinduced electron transfer (PET).[18–20] These azamacrocycle groups act as receptor units for the Zn^{2+} ion, and after coordination, a dramatic increase in the photoluminescence emission occurs as PET quenching is deactivated. However, in addition to the changes in the steady-state emission, the PL decay traces of QD have also been modified after assembly. In agreement with previous reports,[9,21] QD nanoparticles showed long decay times and multi-exponential behaviour. The best fits of the PL decay traces of **QD–MPA** required a sum of three exponential functions (Tables S1 and S2 for **QD_{520}–MPA** and **QD_{600}–MPA**, respectively, ESI†) to reach low χ^2 values, as well as random distributions of the weighted residuals and auto-correlation function, which are indicators of the goodness of the fits. Prior to the immobilization of the azacycle, the intensity-weighted average PL lifetimes, τ_{ave} (see Methods of analysis in the ESI†), of **QD_{520}–MPA** and **QD_{600}–MPA** were 15.8 ± 0.1 and 18.4 ± 0.1 ns, respectively. The three individual decay time components, as well as the average PL lifetime of both the QDs, gradually decreased by increasing the concentration of the azacycle attached on the surface as a result of the PET mechanism (Tables S1 and S2, ESI†). After attachment of the optimized amount of azacycle **1** or **2** on the surface of **QD_{520}–MPA** to obtain the proposed conjugates (see Experimental section in ESI†), the calculated τ_{ave} decreased to 8.6 ± 0.1 ns (**QD_{520}–1**) or 12.0 ± 0.1 (**QD_{520}–2**) (Fig. S1, ESI†). For **QD_{600}–MPA**, the corresponding QD–azacycle showed a decrease in τ_{ave} down to 9.2 ± 0.1 ns or 13.2 ± 0.2 ns for **QD_{600}–1** or **QD_{600}–2**, respectively (Fig. S1, ESI†).

Taking into account that the azacycles can coordinate some metals, the proposed QD–azacycle conjugates show a response in the presence of metals with d^{10} electronic configuration, such as zinc.[18] Indeed, an enhancement of the emission intensity[20] and the average lifetime of QDs were detected upon the addition of Zn^{2+} as a result of the interruption of the PET mechanism between the QD and azacycle (Fig. 1b). The three individual decay time components of the QD–azacycle conjugates were gradually augmented when the concentration of Zn^{2+} of the medium increased (Tables S1 and S2, ESI†). The τ_{ave} of the QD–azacycle conjugates showed a dependency on the concentration of Zn^{2+} with a linear response *versus* the logarithm of the concentration in a range covering approximately three orders of magnitude, between 2 μM and 1 mM for **QD_{600}–1** and between 10 μM and 1 mM for **QD_{520}–2** conjugates (Fig. 1c and d). These ranges suggest the potential application of zinc detection in some Zn^{2+}-rich intracellular media, such as brain tissue.[22] The range of values (10–16 ns) and variation of the PL average lifetime make these nanosensors much more sensitive than previously published fluorescence lifetime probes. For instance, changes of 0.4 ns are usually reported for fluorescence protein-[23] or organic fluorophores-based FLIM sensors.[24] In some occasions, FRET-based FLIM sensors have been reported to work with a total change in the sensor's lifetime as low as 0.06 ns.[25] Our family of QD–azacycle conjugates exhibit a sensitivity that is between 10 and 100 times those figures.

The response of the QD–azacycle conjugates toward Zn^{2+} was in the μM concentration range, with a higher sensitivity of the **QD–1** conjugates than that of the **QD–2** conjugates. This is in agreement with the fact that the binding constant of Zn^{2+} with cyclen **1** is higher than the corresponding binding constant for cyclam **2**.[26] Nevertheless, the response towards Zn^{2+} shown by the QDs of different wavelengths coupled to the same azacycle was very similar, suggesting that the PET mechanism does not depend on the QD size and allowing for the use of different QD conjugates depending on the spectral needs. When compared to other Zn^{2+} sensors, the response of our QD–azacycle conjugates are comparable to other sensors in which the dissociation constant, K_d, of the sensor with the metal ion is in the μM range. The commercially available FluoZin-1 and Newport Green exhibit K_d values in this range,[17] and hence, response to μM concentrations of Zn^{2+}. These commercial sensors are fluorescent indicators with a single Zn^{2+} binding site (1 : 1). They can be responsive to a Zn^{2+} variation along two orders of magnitude (around pK_d ± 1). Hence, increasing the linear range for Zn^{2+} quantitation can only be performed with multiple binding sites. In our case, as each QD contains several azacycle units, the quantitation range reaches almost three orders of magnitude. Newly designed PET sensors have decreased the interaction K_d of Zn^{2+} into the nanomolar range,

allowing for an enhanced sensitivity and quantitation of sub-micromolar Zn^{2+} levels.[27,28] Commercially available FluoZin-3 exhibits a K_d value around 15 nM.[17] However, in such cases, saturation is reached at lower Zn^{2+} concentrations, leading to unsuitable sensors for high Zn^{2+} levels. This situation establishes the need for a careful selection of the suitable fluorescent sensor, depending on the aimed concentration levels of analyte.

The selectivity of the Zn^{2+} nanosensors was also considered in the presence of other metals and molecules that can be found in biological samples. **QD–1** and **QD–2** conjugates were exposed to several potential interfering agents at different concentrations, and the PL decay traces were collected. Fig. S2 (ESI†) shows a summary of the potential interfering species that were tested with no effect in the average PL lifetime of QDs. The τ_{ave} of the proposed nanosensors showed negligible response toward the major intra- and extracellular cations (Na^+, K^+, Ca^{2+} and Mg^{2+}). Metals such as Fe^{2+}, Fe^{3+}, Co^{2+} or Cu^{2+} produce some quenching of the photoluminescence of **QD–MPA** due to some adsorption and inner filter effects;[29] thus, this effect was also detected with the QD–azacycle conjugates. Fig. S2 (ESI†) show the maximum concentration of such interferents that has no effect on the nanosensor τ_{ave}. All these interferents are commonly found in other Zn^{2+} sensors, such as commercial FluoZin-3 or Newport Green.[30] Other transition metals, such as Ni^{2+} or Mn^{2+}, could also coordinate into the azacycle,[31] slightly affecting the τ_{ave} of the QDs. However, these free metal cations are not present, to a large extent, in the majority of biological systems; thus, not representing a major issue for the use of these nanosensors in physiological samples. Moreover, the effect of changes in the pH value of the medium in the response of the Zn^{2+} nanosensors was also evaluated. The pH value may have an effect because it alters the coordination efficiency of the azacycles toward Zn^{2+}, and because of the presence of remaining free carboxylic groups on the surface from non-reacted MPA. Nevertheless, at the different pH tested, the τ_{ave} of the QD–azacycle conjugates after reaction with 0.1 mM Zn^{2+} increased a similar amount (55% at pH 5.47, 65% at pH 6.49, and 47% at pH 7.20, Fig. S3, ESI†), indicating that the Zn^{2+} response was not altered. Therefore, the pH of the medium must be known and controlled while determining Zn^{2+} concentrations with the proposed conjugates.

We tested the usefulness of the QD–azacycle nanosensors for the detection of Zn^{2+} concentrations by employing FLIM imaging, especially in intracellular applications. First, **QD_{600}–1** nanosensors dissolved in 10 mM TRIS buffer at pH 7.2 with different Zn^{2+} concentrations and deposited on a glass slide were imaged using a confocal FLIM microscope. The increase in the τ_{ave} with increasing concentrations of Zn^{2+} was visible in the arbitrary colour scale image, as well as in the lifetime distributions obtained upon analysis of the images (Fig. 2). These results suggested that the proposed nanosensors could be promising as FLIM-based intracellular Zn^{2+} probes.

The **QD–1** nanosensors were introduced into live HepG2 cells for intracellular Zn^{2+} sensing. After the incubation, the cells internalized the nanoparticles mainly by cellular

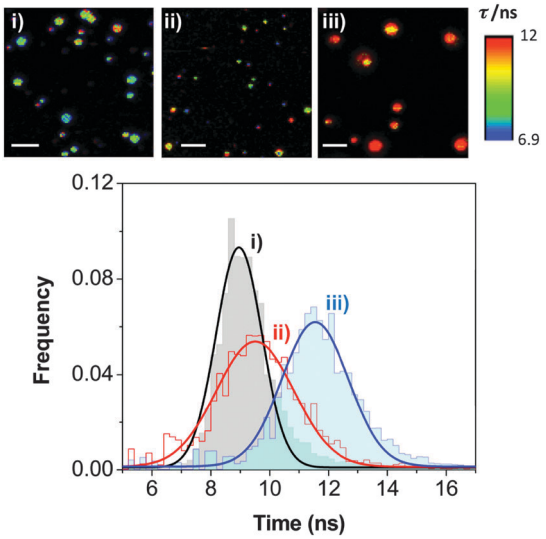

Fig. 2 FLIM images and the corresponding lifetime distributions of **QD_{600}–1** conjugates suspended in 10 mM Tris buffer pH 7.2 deposited on glass slides in the presence of different concentrations of Zn^{2+}: (i) 0 mM Zn^{2+}; (ii) 0.1 mM Zn^{2+}; and (iii) 1 mM Zn^{2+}. White scale bars represent 5 μm.

endocytosis (Fig. S4, ESI†). After the 2 hour of incubation time, the QDs exhibited negligible toxicity on the cells (see ESI† and Fig. S5 for survival rates). Fig. 3 shows FLIM images of **QD_{600}–1** in the absence and presence of 1 mM Zn^{2+}. The images show an enhancement of the average PL lifetime of QDs in cells treated with Zn^{2+}. The changes in the PL lifetime distributions of the regions of interest indicate the excellent response of the proposed QD lifetime-based nanosensors inside the cells. It is important to note that the long-lived PL of the QD nanosensors can be easily distinguished from the interfering cellular

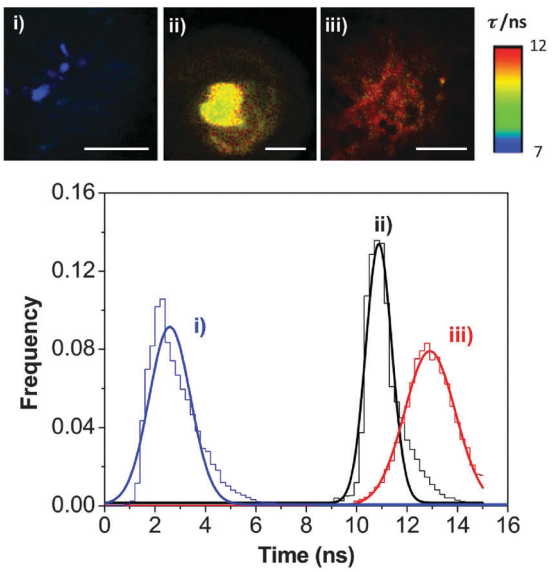

Fig. 3 FLIM images and the corresponding lifetime distributions of HepG2 cells in PBS pH 8.0: (i) autofluorescence; (ii) cells with **QD_{600}–1** conjugates; (iii) cells with **QD_{600}–1** conjugates incubated with 1 mM Zn^{2+}. White scale bars represent 5 μm.

autofluorescence. In the absence of QDs, the cells displayed minimal emission with lifetimes of approximately 2.6 ns (Fig. 3). In contrast, the τ_{ave} associated with the QDs was significantly longer than that of cell autofluorescence, even in the absence of Zn^{2+}. The commercial probe, Newport Green, has been previously used to measure intracellular Zn^{2+} levels using phase-modulation FLIM,[32] with the fluorescence lifetime increasing from 0.88 to 2.93 ns; values which lie in the same range than cellular autofluorescence, presumably causing interferences. The use of the long lifetime of the QD sensors is a much more powerful approach, as the cell autofluorescence is discarded by applying suitable time windows.

In conclusion, we have demonstrated the advantages of the FLIM methodology, particularly in combination with QD nanoparticles, whose very long PL lifetime greatly enhances the sensitivity and selectivity of the nanosensors. These long decay times facilitate the discrimination between the signal from the sensor and the intrinsic fluorescence of the cells and produce an enhanced signal-to-background ratio. Moreover, the FLIM technique also eliminates the need for a near-infrared probe because it can use fluorophores with emission within the range of the green cellular autofluorescence. However, all of these excellent advantages have not yet been exploited because recently, only a couple of studies using the combination of QDs and FLIM microscopy have been published.[4,15] Nevertheless, those works are aimed at pH sensing. To the best of our knowledge, this is the first time that QD-based FLIM sensors are specifically designed for intracellular detection of an important metal ion. This methodology can be extended to the development of other nanosensors for the detection of a wide range of molecules of interest. Other photophysical processes, such as charge transfer or energy transfer (FRET), that may take place at the QD surface with other ligands have an effect on the PL decay time.[9] Any of these processes can be optimized for developing specific FLIM nanosensors. Nevertheless, for intracellular application, special attention to excessive aggregation or cell intake must be taken into account.

This work was supported by Fundación Ramon Areces and grant CTQ2014-56370-R from Ministerio de Economia y Competitividad of Spain. We also thank Dr M. D. Giron and Dr R. Salto for kindly supplying the cell cultures.

Notes and references

1 M. J. Ruedas-Rama, J. D. Walters, A. Orte and E. A. H. Hall, *Anal. Chim. Acta*, 2012, **751**, 1–23.
2 A. P. Alivisatos, W. Gu and C. Larabell, *Annu. Rev. Biomed. Eng.*, 2005, **7**, 55–76.
3 U. Resch-Genger, M. Grabolle, S. Cavaliere-Jaricot, R. Nitschke and T. Nann, *Nat. Methods*, 2008, **5**, 763–775.
4 A. Orte, J. M. Alvarez-Pez and M. J. Ruedas-Rama, *ACS Nano*, 2013, **7**, 6387–6395.
5 R. Freeman, R. Gill, I. Shweky, M. Kotler, U. Banin and I. Willner, *Angew. Chem., Int. Ed.*, 2009, **48**, 309–313.
6 Y. Wang, H. Mao and L. B. Wong, *Talanta*, 2011, **85**, 694–700.
7 Y.-S. Liu, Y. Sun, P. T. Vernier, C.-H. Liang, S. Y. C. Chong and M. A. Gundersen, *J. Phys. Chem. C*, 2007, **111**, 2872–2878.
8 M. Ruedas-Rama, J. Alvarez-Pez, L. Crovetto, J. Paredes and A. Orte, in *Advanced Photon Counting*, ed. P. Kapusta, M. Wahl and R. Erdmann, Springer International Publishing, 2015, pp. 191–223.
9 M. J. Ruedas-Rama, A. Orte, E. A. H. Hall, J. M. Alvarez-Pez and E. M. Talavera, *ChemPhysChem*, 2011, **12**, 919–929.
10 M. J. Ruedas-Rama, A. Orte, E. A. H. Hall, J. M. Alvarez-Pez and E. M. Talavera, *Chem. Commun.*, 2011, **47**, 2898–2900.
11 M. J. Ruedas-Rama, A. Orte, E. A. H. Hall, J. M. Alvarez-Pez and E. M. Talavera, *Analyst*, 2012, **137**, 1500–1508.
12 J. U. Sutter, D. J. S. Birch and O. J. Rolinski, *Meas. Sci. Technol.*, 2012, **23**, 055103.
13 R. K. Pai and M. Cotlet, *J. Phys. Chem. C*, 2011, **115**, 1674–1681.
14 L. Carlini and J. L. Nadeau, *Chem. Commun.*, 2013, **49**, 1714–1716.
15 C. Chen, P. Zhang, L. Zhang, D. Gao, G. Gao, Y. Yang, W. Li, P. Gong and L. Cai, *Chem. Commun.*, 2015, **51**, 11162–11165.
16 T. Fukada, S. Yamasaki, K. Nishida, M. Murakami and T. Hirano, *J. Biol. Inorg. Chem.*, 2011, **16**, 1123–1134.
17 L. Zhu, Z. Yuan, J. T. Simmons and K. Sreenath, *RSC Adv.*, 2014, **4**, 20398–20440.
18 E. G. Moore, P. V. Bernhardt, A. Fürstenberg, M. J. Riley, T. A. Smith and E. Vauthey, *J. Phys. Chem. A*, 2005, **109**, 3788–3796.
19 P. V. Bernhardt, E. G. Moore and M. J. Riley, *Inorg. Chem.*, 2002, **41**, 3025–3031.
20 M. J. Ruedas-Rama and E. A. H. Hall, *Anal. Chem.*, 2008, **80**, 8260–8268.
21 M. Dahan, T. Laurence, F. Pinaud, D. S. Chemla, A. P. Alivisatos, M. Sauer and S. Weiss, *Opt. Lett.*, 2001, **26**, 825–827.
22 C. J. Frederickson, J.-Y. Koh and A. I. Bush, *Nat. Rev. Neurosci.*, 2005, **6**, 449–462.
23 M. Tantama, Y. P. Hung and G. Yellen, *J. Am. Chem. Soc.*, 2011, **133**, 10034–10037.
24 J. M. Paredes, M. D. Giron, M. J. Ruedas-Rama, A. Orte, L. Crovetto, E. M. Talavera, R. Salto and J. M. Alvarez-Pez, *J. Phys. Chem. B*, 2013, **117**, 8143–8149.
25 C. D. Harvey, A. G. Ehrhardt, C. Cellurale, H. Zhong, R. Yasuda, R. J. Davis and K. Svoboda, *Proc. Natl. Acad. Sci. U. S. A.*, 2008, **105**, 19264–19269.
26 M. Kodama and E. Kimura, *J. Chem. Soc., Dalton Trans.*, 1977, 2269–2276.
27 J. Fan, X. Peng, Y. Wu, E. Lu, J. Hou, H. Zhang, R. Zhang and X. Fu, *J. Lumin.*, 2005, **114**, 125–130.
28 M. Taki, J. L. Wolford and T. V. O'Halloran, *J. Am. Chem. Soc.*, 2004, **126**, 712–713.
29 Y. Chen and Z. Rosenzweig, *Anal. Chem.*, 2002, **74**, 5132–5138.
30 J. Zhao, B. A. Bertoglio, M. J. Devinney Jr, K. E. Dineley and A. R. Kay, *Anal. Biochem.*, 2009, **384**, 34–41.
31 S. Mossin, H. O. Sørensen, H. Weihe, J. Glerup and I. Søtofte, *Inorg. Chim. Acta*, 2005, **358**, 1096–1106.
32 R. B. Thompson, D. Peterson, W. Mahoney, M. Cramer, B. P. Maliwal, S. W. Suh, C. Frederickson, C. Fierke and P. Herman, *J. Neurosci. Methods*, 2002, **118**, 63–75.